

## ON THE POTENTIAL OF NEW DIGITAL AERIAL CAMERAS FOR DEM GENERATION

Joachim Höhle

Aalborg University, Department of Planning, Denmark

jh@land.aau.dk

### **ABSTRACT**

*Based on practical experiences with the first generation of digital cameras, the impact of new digital aerial cameras on the generation of digital elevation models is estimated. The new cameras are evaluated with respect to elevation accuracy, area coverage and image quality. The produced tables and graphs show the potential of the new cameras regarding the accuracy of automatically derived elevations. For better elevation accuracy, the increases of the base/height ratio and of the resolving power of lenses are more important than the reduction of the pixel size. The impact of multi-ray photogrammetry, sensors for georeferencing, multi-spectral images and new matching algorithms is also discussed. All of the mentioned innovations will improve the accuracy of DEMs derived by photogrammetry.*

### **1. INTRODUCTION**

During the last 10 years the production of digital elevation models has become completely digital and to a large extent automatic. The appearance of digital aerial cameras is one of the reasons for this success. Several manufacturers have recently announced new large-format frame cameras. Their potential with regard to the elevation accuracy is of interest to the mapping industry. The format of the selected cameras is very different. It may be composed of several CCDs belonging to different cameras. Also, the size of the pixel differs in the new cameras. The lenses applied in the cameras have different focal length and quality. The georeferencing of the images is also important for good elevation accuracy. New sensors for position and attitude and reliable calibration of the acquisition system are equally important. The processing of the images to DEMs can also be improved thanks to the multispectral capability of new cameras and new approaches in matching and filtering. All of these parameters and changes in the methodology will influence the elevation accuracy of the photogrammetric method. In the following, the potential of four new large-format frame cameras regarding DEM generation will be discussed. It is an objective of this contribution to analyse the influencing factors and to predict the results regarding the elevation accuracy at DEM generation with this type of cameras.

### **2. FOUR NEW LARGE-FORMAT FRAME CAMERAS**

The innovations in the four large-format frame cameras, first of all, concern the number of pixels per image. It now reaches up to 260 million pixels (Megapixel) in the UC Eagle. The side of the squared pixel is as small as 5.2  $\mu\text{m}$ . Another rather new camera of the same company, Microsoft/Vexcel Imaging, is the UC-Xp WA. The applied lens has a big field of view and is thereby especially suitable for DEM generation. Both cameras are described in (Gruber et al., 2011). The new camera of Hexagon/Intergraph uses one large CCD only which prevents the fusion of several

images into one image of a larger format (Neumann, 2011). The image size in flight direction of the DMCII-250 has now 14656 pixels corresponding to 82.1 mm. Detailed information on the fourth new camera, IGI 235 of IGI mbH, is contained in (Minten, 2011). General information on digital aerial cameras may be read in (Sandau, 2005). Table 1 contains these four new frame cameras with their features which have influence on the geometric accuracy.

Table 1. Features of four new digital aerial cameras

<i>Features</i>	<i>IGI 235</i>	<i>UC-Xp WA</i>	<i>UC Eagle</i>	<i>DMCII 250</i>
<i>pixel size [<math>\mu\text{m}</math>]</i>	6	6	5.2	5.6
<i>focal length [mm]</i>	80	70	80	112
<i>image size (in flight direction) [pel]</i>	12 750	11 310	13 080	14 656
<i>[mm]</i>	76.50	67.86	68.02	82.07
<i>image size (across flight direction)[pel]</i>	18500	17310	20010	17216
<i>[mm]</i>	111.0	103.9	104.1	96.4
<i>base/height ratio at p=60%</i>	0.38	0.39	0.34	0.29

If the images have the standard forward overlap of  $p = 60\%$ , the image base is  $b' = 0.4 \cdot s'_{\text{fld}}$ , where  $s'_{\text{fld}} =$  image size in flight direction. From Table 1, it can be noticed that the base/height ratio is highest for the UC-Xp WA camera and lowest for the DMC-250 camera. The older digital cameras have smaller base/height ratios: 0.27 (UC-D) and 0.31 (DMC). Other camera features like frame rate and image quality have also influence on the geometric quality of the DEM and will also be dealt with in the following.

### 3. FEATURES WHICH INFLUENCE THE GEOMETRIC ACCURACY OF DEMS

Besides the camera, there are other features which influence the geometric accuracy of DEMs. Sensors which determine the position and attitude of the camera as well as the processing of the data are important too. The accuracy of elevations also depends of the terrain type. These last influences can only be presented in an overview. Investigations dealing with the DEM accuracy will be mentioned.

#### 3.1 Geometric accuracy of the cameras

The performance of digital aerial cameras has been investigated by several research groups, for example Jacobsen (2011), Haala et al. (2010), Spreckels et al. (2010), Höhle (2009a; 2009b), and Honkavaara et al. (2006). Besides the camera, also the flight parameters (altitude, side lap) and the processing tools influence the accuracy of the derived elevations. Furthermore, the terrain type, the density and the definition of the points have an effect. The assessment of the accuracy needs checkpoints of superior accuracy. The applied accuracy measures should not be affected by blunders.

In the investigation of the DMCII-140, which uses one 140Mpixel CCD with a  $7.2 \mu\text{m} \times 7.2 \mu\text{m}$  large pixel, a vertical accuracy of  $\text{RMSE}_h = 0.7 \cdot \text{GSD}$  (ground sample distance) has been achieved for well-defined checkpoints using semi-automated measurements (Jacobsen, 2011). The imagery used 65% forward overlap and 65% side overlap, and the determination of the check and control

points could in average use seven images. The object points have been determined within an aerotriangulation. The achieved high accuracy is, however, not a result of a DEM generation.

In tests of a project group of the German society of photogrammetry, remote sensing and geoinformation (DGPF), it was found that the generation of very dense DEMs by means of the DMC images with GSDs of 8 cm and 20 cm could be done with  $RMSE_h = 0.4 \cdot GSD$  and  $RMSE_h = 0.8 \cdot GSD$ , respectively (Haala et al., 2010). The checkpoints were well-defined and with good contrast to the surroundings, and the derived DEM had a very narrow spacing of the grid points. A few blunders were eliminated by a threshold ( $3 \cdot RMSE$ ). High elevation accuracies of  $\sigma_h = 0.45 \cdot GSD$  were obtained when well-defined points were manually measured in DMC images by an experienced operator (Spreckels et al., 2010). Other investigations were carried out in (Höhle, 2009a; 2009b) using UltraCam-D and DMC images. In order to estimate the results with the new cameras, the factors influencing the accuracy have to be known. In general, the estimates of the elevation accuracy can be calculated after the equation (1).

$$\sigma_h = \frac{h}{b} \cdot \sigma_{px'} \cdot m_b \quad (1)$$

where  $\sigma_h$  = elevation accuracy,  $h$  = (average) flying height above ground,  $b$  = base,  $\sigma_{px'}$  = parallax accuracy related to the image, and  $m_b$  = image scale figure.

The formula can be ‘modernized’ with regard to digital cameras:

$$\frac{\sigma_h}{GSD} = \frac{f}{b'} \cdot \frac{\sigma_{px'}}{pel'} \quad (2)$$

$$GSD = pel' \cdot m_b = pel' \cdot \frac{h}{f}$$

where  $f$  = focal length and  $pel'$  = pixel size in image.

The elevation accuracy may also be related to the flying height above ground by

$$\frac{\sigma_h}{h} = \frac{\sigma_{px'}}{b'} \quad (3)$$

The image base ( $b'$ ) may be determined from the number of pixels in the direction of flight ( $s'_{fld}$ ) assuming 60% forward overlap. The accuracy of parallaxes ( $\sigma_{px'}/pel'$ ) can empirically be derived by means of equation (4).

$$\frac{\sigma_{px'}}{pel'} = \frac{b'}{f} \cdot \frac{\sigma_h}{GSD} \quad (4)$$

In (Höhle, 2009b) the parallax accuracy has been derived for the DMC camera (cf. Table 2). The required value for the accuracy ( $\sigma_h$ ) has been found through a comparison with accurate reference points. The mean of the parallax accuracy is 0.36 pixels. This value is independent of the used overlap. It should be a constant value for the DMC camera provided that the orientation of the images is error-free and the terrain is not covered with vegetation or buildings. Other cameras may have other values. For example, in (Höhle, 2009a) the parallax accuracy has been determined for the UC-D camera ( $f = 101\text{mm}$ ,  $pel' = 9 \mu\text{m}$ ,  $b/h = 0.27$  at  $p = 60\%$ ,  $s'_{fld} = 7500$

pixel) under similar conditions ( $GSD = 6 \text{ cm}$ ,  $p = 60\%$ ,  $q = 20\%$ , processing with Match-T), and the parallax accuracy has been  $\sigma_{px'} = 0.67$  pixels corresponding to  $6.0 \mu\text{m}$ . The average from all three tests using large format cameras of the first generation is  $(\sigma_{px'})_{\text{average}} = 0.46 \approx 0.5$  pixels.

*Table 2. Results of automatic DTM derivation in open terrain using the DMC camera ( $f = 120 \text{ mm}$ ,  $pel' = 12 \mu\text{m}$ ,  $s'_{fld} = 7680 \text{ pixel}$ ,  $b/h = 0.31$  at  $p = 60\%$ ), standard overlap ( $p = 60\%$ ,  $q = 20\%$ ) and processing with Match-T.*

$b/h$	$GSD$ [cm]	spacing [m]	$\sigma_h$ [cm]	$\sigma_h$ [GSD]	$\sigma_{px'}$ [pixels]
0.31	20	3.0	17.0	0.85	0.26
0.31	10	1.6	15.0	1.50	0.46

In the following accuracy estimation for the four new cameras it is assumed that the parallax accuracy is  $\sigma_{px'} = 0.5$  pixels as well. Table 3 displays the estimated elevation accuracy which the four new cameras may achieve. It is calculated by equations 2 and 3, respectively. In addition, the results for cameras of the first generation are given as reference. From Table 3 can be read that  $\sigma_h/h$  will improve at all of the new cameras. The estimated elevation accuracy expressed in GSD units with the DMCII-250 is not better than the results with the DMC. When mass points for the purpose of terrain modelling are automatically determined the terrain type will have influence. Terrain areas with buildings and vegetation have to be filtered and arising gaps must be closed by interpolation. Errors will occur in these processes and the obtainable accuracy is then less than in open terrain.

*Table 3. Estimated elevation accuracy of new digital cameras (using parallax accuracy of  $\sigma_{px'} = 0.5$  pixels and forward overlap  $p = 60\%$ ).*

Camera	estimated elevation accuracy	
	[% of h]	[GSD]
UC-D	0.17	1.87
DMC	0.16	1.63
IGI 235	0.10	1.31
UC-Xp WA	0.11	1.29
UC Eagle	0.10	1.47
DMCII 250	0.09	1.71

It has to be assumed that some of the new cameras have a higher geometric accuracy than the older cameras. Practical tests will be necessary in order to derive reliable values of the parallax accuracy for each of the new cameras.

### 3.2 Coverage in object space

Due to a newly designed lens the format of the CCD in the DMCII-250 is completely used for imaging. The ground coverage (foot print) at  $GSD = 10 \text{ cm}$  is  $1722 \text{ m} \times 1466 \text{ m}$  or  $2.52 \text{ km}^2$ . The foot prints of the UC Eagle and of the IGI-235 cameras (both equipped with an 80 mm lens) cover about the same area; but the UC-Xp-WA camera covers only 78% of the area of the DMCII-250 at the same GSD. The image size across the direction of flight (swath width) determines the number stripes to be flown. The swath width of the DMCII-250 at  $GSD = 10 \text{ cm}$

is 1722 m (cf. Table 1) and thereby smallest among the four new cameras. A big swath width is important for the economy in image taking.

### 3.3 Increase of overlap and combined use of imagery

The accuracy can be improved when the elevations are determined from several images. This multi-ray approach is achieved by higher overlaps. The increase of the forward overlap to 80% is achieved almost without additional costs. The small frame rate of the new cameras, e.g. 1.7 seconds at the DMCII-250, makes a ground resolution of GSD = 5cm possible at ground speeds of the aircraft up to 310 km/h. Figure 1 depicts an image together with the centres of four overlapping images, and Table 4 shows the base/height ratio and the convergence angle for various combinations of image pairs. The elevations are derived from image pairs and have to be merged or the intersection of points is carried out simultaneously from several images. Special software for the processing is then necessary and also available from different vendors, e.g. Erdas and Inpho. Using several photogrammetric models and merging the derived DEMs will reduce the number of blunders and improve the accuracy. The accuracy is also improved by means of higher side overlap, e.g. of  $q = 60\%$ . However, this approach increases the costs of flying. The use of imagery of different overlap has an effect on the precision of matching. Generally, a large base line leads to differences in the perspective distortion, which may create blunders at large scale imagery. In contrast, a small base line will improve the matching precision, but the elevation accuracy will suffer due to the unfavourable base/height ratio.

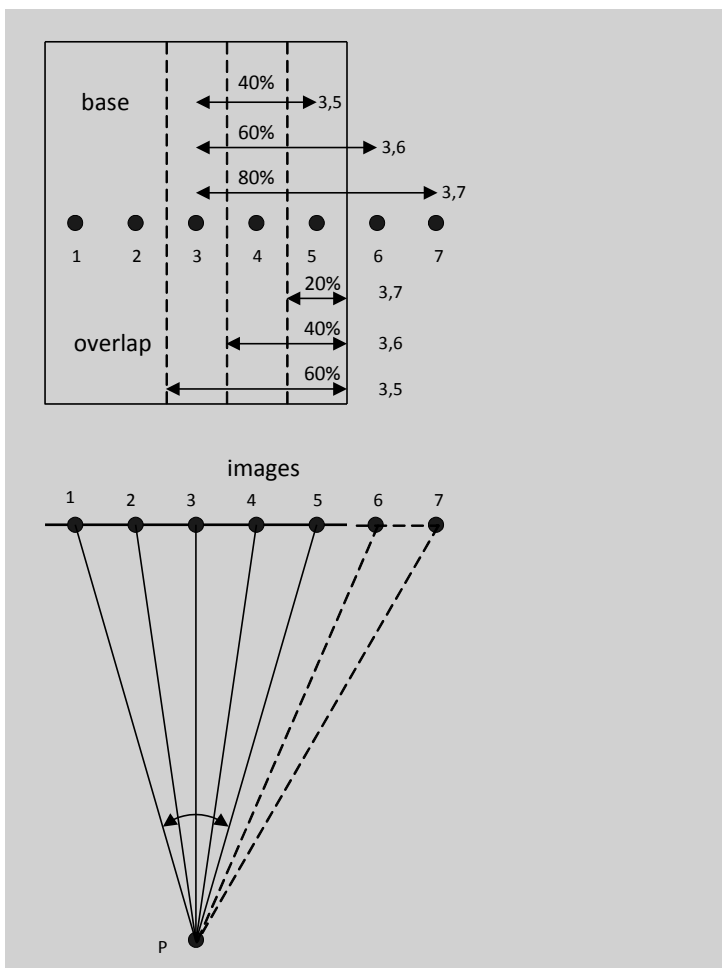


Figure 1. Multiple image pairs may be used to determine the elevation of an object point (P). For image pairs with less overlap the base/height ratio is increased and the accuracy of the derived elevations is improved.

It means:  $\gamma =$  convergence angle.

Table 4. Overlap, base/height ratios, and convergence angle at different image pair combinations of the digital large format camera DMC II-250.

Image pair	overlap [%]	base/height ratio	convergence angle [gon]
1,5/3,7	20	1/1.7	36
1,4/2,5/3,6	40	1/2.3	27
1,3/2,4/3,5	60	1/3.4	18
1,2/2,3/3,4/4,5	80	1/6.8	9

### 3.4 Image quality

Important for good results in geometry is also the quality of the produced image. A small GSD enables detection of small objects and high pointing accuracy when measuring image coordinates. Figure 2 compares the new cameras with respect to GSD at a certain flying altitude. The DMC II 250 produces the smallest GSD. However, the DMCII-250 has to be flown at higher altitudes in order to achieve the same GSD (cf. Figure 3). This fact will reduce contrast and colour balancing in the images. The camera has a high dynamic range (>70dB) and details in shadows can therefore be seen. All digital aerial cameras are tolerant to underexposure (Sandau, 2005).

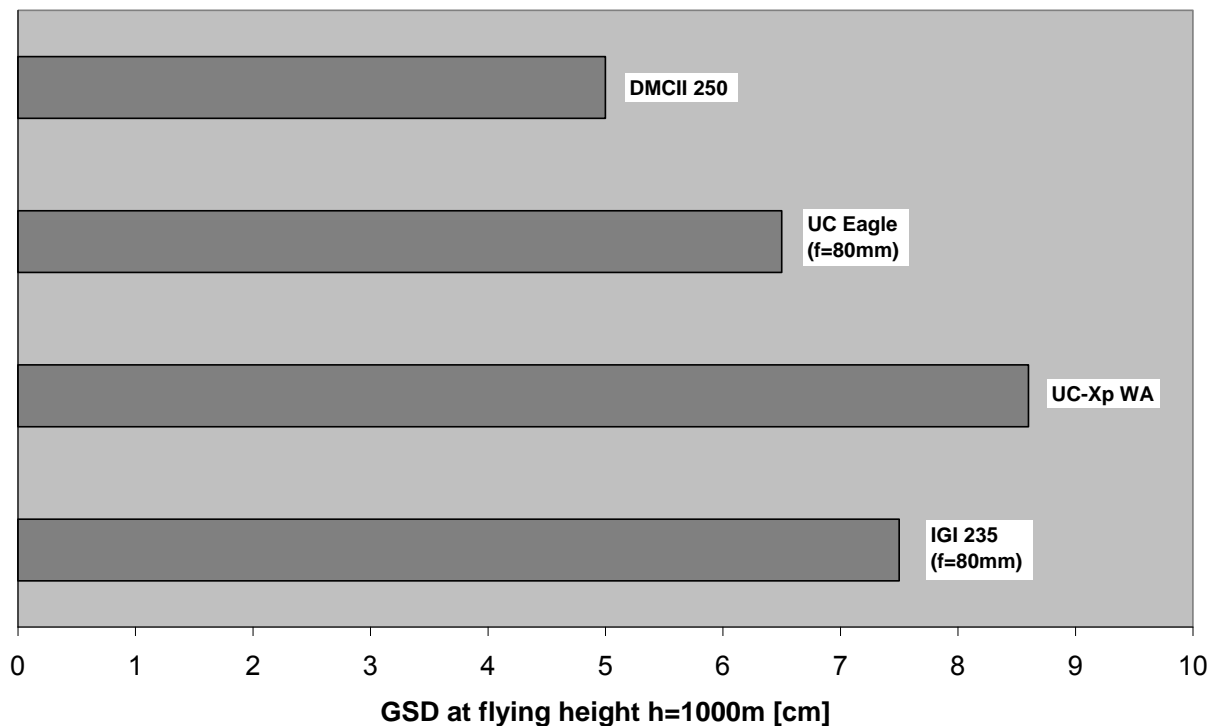


Figure 2. Ground sampling distance (GSD) for the new cameras

The size of the pixel is not the only criterion for high image quality. The resolving power of the lens has to be equally high. A CCD with pixels of  $5.6 \mu\text{m} \cdot 5.6 \mu\text{m}$ , for example, requires a lens with a resolution of  $R = 1000 / (2 \cdot 5.6 \mu\text{m}) = 89$  line pairs per mm (lp/mm). The resolution of the lens is not constant; it decreases from the middle of the lens to the corners. Furthermore, diffraction will occur when high f-numbers have to be used for correct exposures. The DMCII-250 camera is equipped with a new lens which matches the small pixel size.

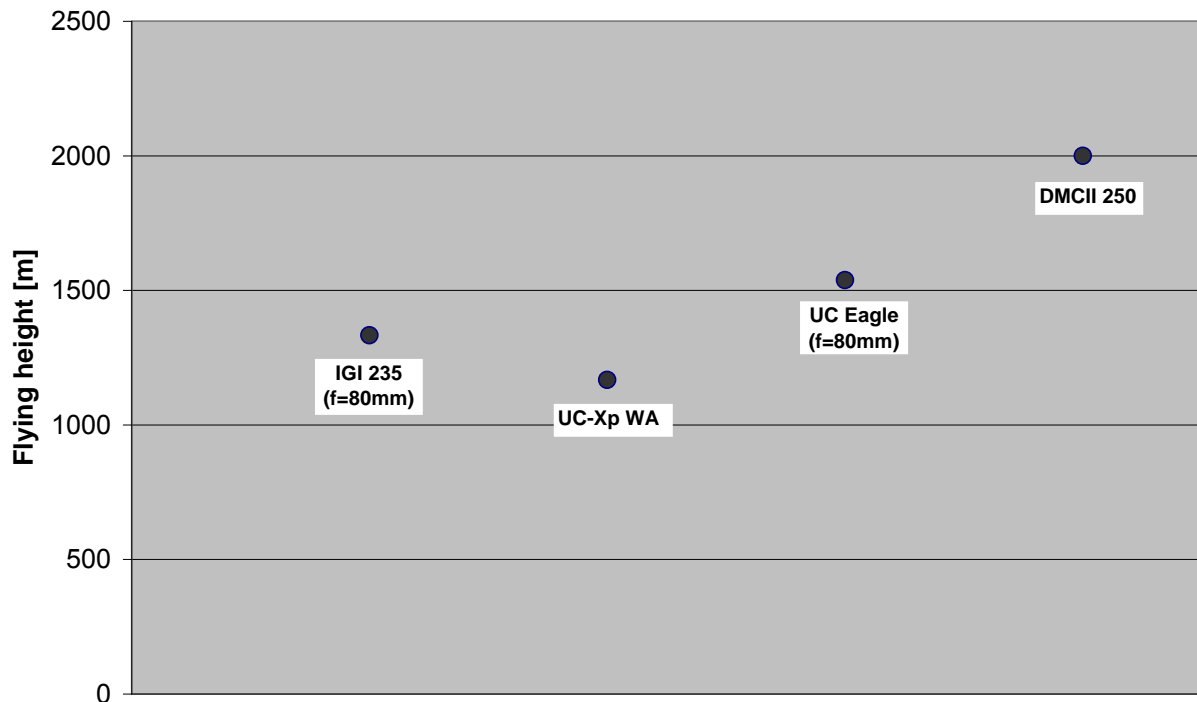


Figure 3. Flying height at GSD = 10cm.

A filter removes light beyond the wavelength of  $\lambda = 710\text{nm}$ . The IGI-235 (also called Quattro DigiCAM) has interchangeable lenses with focal lengths of  $f = 80, 100, \text{ and } 150 \text{ mm}$ . The UC Eagle can also be used with a 210 mm lens. DEM generation is best done with wide angle lenses. The forward image motion due to speed of the aircraft has to be compensated; it is done in three of the four cameras by time-delayed integration (TDI). The IGI 235 reduces motion blur by means of short exposure time and extended radiometric range. This technique is named “Blur Management Control” (BMC). The new generation cameras use 14 bit for the analogue/digital conversion. Such a radiometric resolution means that 16384 intensity values (digital numbers) are possible. The post processing, which comprises corrections, fusion and pan sharpening, is carried out even in higher radiometric resolutions. The UC Eagle, for example, carries out this post processing in 16 bit. All manufacturers use special methods to maintain the dynamic range in the scene. The photogrammetric processing by the user is often carried out with compressed data. High compression factors and use of data with 8 bit per channel will lead to loss of information. 16 bit per channel and 64 bit computers are recommended for the generation of high-quality DEMs. It is obvious from the foregoing description that the image quality has a big influence on the DEM accuracy.

### 3.5 Multi-spectral capability

The images of the mentioned cameras can be black & white, colour or colour infra-red (false colour) images. In the case of DMCII-250, UC-Xp WA and UC-Eagle the colour and colour infra-red images are produced by means of pan-sharpening from four multi-spectral cameras of lower resolution and smaller focal length. The PAN/colour ratio is 1:3.2 for the DMCII-250 and 1:3.0 for the UC-Eagle and UC-Xp WA. The IGI Quattro DigiCAM produces the colour and false colour by means of mosaic filters and Bayer interpolation. By means of colour, the interpretation of objects can be done much more efficiently and reliably in manual processes. Also automated procedures for classification can take advantage of the multi-spectral capability of the new cameras. This and other remote sensing methods require a radiometric calibration of

the camera. Details are dealt with e.g. in (Honkavaara et al., 2009). The use of multispectral imagery in DEM production and updating of databases has been demonstrated in (Champion, 2009).

### **3.6 Sensors for georeferencing of images**

The exterior orientation of the images determines the accuracy of the DEM to a great extent. The use of ground control is expensive and the number of ground control points therefore has to be reduced to a minimum. A global positioning device (GNSS) and an inertial measuring unit (IMU) are added to the camera and an integrated sensor orientation is carried out. That means that the observations of these positional sensors are used together with the measured image coordinates in a combined adjustment. The connection of the images by means of automatically measured tie points is a strong feature of this “photogrammetric georeferencing”. Very accurate results for the exterior orientation, and thereby for the DEM, can then be obtained. Another prerequisite is the calibration of the camera and the relative orientation between all sensors (bore sight misalignment). They are determined in situ, that means in a test flight. The existence of a test field is then another prerequisite for good results. Details on this integrated sensor orientation are published e.g. in (Heipke et al., 2002).

### **3.7 Processing of images**

The DEM generation is based on matching of image patches. The contents of the images are first reduced to features (distinct points), and correspondence of features in other images is found by comparing their attributes. This so-called feature based matching (FBM) is applied in different levels of an image pyramid. Another matching method, least-squares matching (LSM), is based on intensity values of pixels. Similarity between image patches is found by calculation of correlation coefficients. Sub-pixel values for the position of best fit are found by adjustment. The precision of FBM and LSM is quoted with 0.3 and 0.1 pixels respectively (Trimble/Inpho, 2011). A third method, semi-global matching (SGM), is carried out for each pixel and applies mutual information as similarity measure. After corresponding positions are derived, the 3D coordinates of points are intersected using rays of several images. The derived point cloud is then classified into ground points and elevated points. A digital terrain model (DTM) and a digital surface model (DSM) can be derived. The DTM and the DSM will have a high density (distance between grid points may be as small as one GSD) and they are produced very fast when proper hardware and software are applied. The process is carried out automatically. Mismatches can occur, e.g. due to lack of texture and contrast, big changes in the perspective or at borders of shadows. Filtering for blunders is an important task which needs special strategies. The results of the DEM generation are influenced by the applied software tools and by the selection of the many parameters within these tools. The new tools are described in Hirschmüller (2011), Haala (2011), and Heuchel et al. (2011).

## **4. DISCUSSION**

All four new cameras have a much larger number of pixels per final output image than the first generation cameras. The pixel sizes in all cameras are now very small. Important for the user is the elevation accuracy for a given GSD. The empirical tests of the author with the first generation cameras (DMC and UC-D) revealed parallax accuracies of about 0.5 pixels in average. Applying this value for all of the new cameras the elevation accuracy will then be higher for the large-format cameras (IGI-235 and UC-Xp WA) due to their bigger base/height ratio. The one-chip



camera (DMCII-250) comes close to the results of the large-format camera DMC. It is also advantageous that the elevations can be determined by several images due to the short frame rate in the new cameras. This multi-ray photogrammetry requires higher forward and side overlap and special software packages. Practical experience is still necessary in order to use this approach with its full potential. The productivity of DEM generation will be improved with the four new cameras. The swath width is increased either due to a larger field of view (UC-Xp WA, IGI, 235) or due to a higher flying height (DMCII-250, UC Eagle), which the small pixel or the longer focal length require. The ground resolution, however, will still be high. The high image quality and radiometric resolution of the new digital cameras enable very dense point clouds at automated DEM generation. The terrain can be modelled more accurately. Break lines, buildings and other objects can automatically be extracted more accurately and reliably.

## 5. CONCLUSION

Determination of elevations and DEMs will benefit from using one of the new cameras. The improvements are due to a more favourable base/height ratio or where the fusion of several CCDs is avoided. It is important to understand that a small pixel will not necessarily result in high resolution of the image. The resolution of the lens has to match the resolution of the CCD. Applying a parallax accuracy of  $\sigma_{px} = 0.5$  pixels for all four new cameras, the achievable accuracy can be estimated and compared. In order to obtain a vertical accuracy of  $\sigma_h = 10$  cm, the images have to be taken with a ground sampling distance of GSD = 5.9 cm (DMCII-250), 6.8 cm (UC Eagle), 7.6 cm (IGI-235,  $f = 80$  mm), or 7.8 cm (UC-Xp WA). Other improvements in the positional devices (GNSS/IMU) and the procedures of integrated sensor orientation will contribute to higher DEM accuracies. The ground coverage of the UC Eagle is largest (100%), 96% at the DMCII-250, 90% at the IGI-235 camera (80 mm lens), and 75% at the UC-Xp WA camera when the same ground resolution is maintained. Due to a short frame rate the multi-ray and multi-model techniques can be applied at all new cameras which will further improve the vertical accuracy. Other applications, e.g. the extraction of buildings and the production of true orthoimages, will benefit from the new cameras. Practical tests with the new cameras have now to be carried out in order to confirm these theoretical considerations. With the appearance of the four new aerial large-format frame cameras the development of digital aerial cameras is not finished. The CCDs may become larger and squared and used in single chip or multi-chip designs. The image quality and other features of the cameras will improve in future as well. All this progress in the cameras and the processing tools will definitely improve the DTM/DSM generation by means of photogrammetry.

## 6. REFERENCES

- Champion, N., 2009. Detection of unregistered buildings for updating 2D databases, EuroSDR publication no. 56, pp. 7-54.
- Gruber, M., Ponticelli, M., and Wiechert, A., 2011. UltraCam, a brand for continuous developments, in: Fritsch, D. (Ed.), Photogrammetric Week '11, Wichmann Verlag, ISBN 978-3-87907-507-2, pp. 103-109.
- Haala, N., Hastedt, H., Wolf, K., Ressel, C., Baltrusch, S., 2010. Digital photogrammetric camera evaluation - generation of Digital Elevation Models, PFG 2/2010, pp. 99-115.

- Haala, N., 2011. Multi-ray photogrammetry and dense image matching, in: Fritsch, D. (Ed.), Photogrammetric Week '11, Wichmann Verlag, ISBN 978-3-87907-507-2, pp. 185-195.
- Heuchel, T., Köstli, A., Lemaire, C., Wild, D., 2011. Towards a next level of quality DSM/DTM extraction with Match-T, in: Fritsch, D. (Ed.), Photogrammetric Week '11, Wichmann Verlag, ISBN 978-3-87907-507-2, pp. 197-202.
- Heipke, C., Jacobsen, K. and Wegmann, H. (Eds.), 2002. Integrated sensor orientation, EuroSDR publication no. 43, 297 p.
- Hirschmüller, H., 2011. Semi-global matching – motivation, developments and applications, in: Fritsch, D. (Ed.), Photogrammetric Week '11, Wichmann Verlag, ISBN 978-3-87907-507-2, pp. 173-184.
- Honkavaara, E., Ahokas, E., Hyypä, J., Jaakkola, J., Kaartinen, H., Kuittinen, R., Markelin, L., Nurminen, K., 2006. Geometric test field calibration of digital photogrammetric sensors, ISPRS Journal of Photogrammetry and Remote Sensing, Volume 60, Issue 6, pp. 387-399.
- Honkavaara, E., Arbiol, R., Markelin, L., Martinez, L., Cramer, M., Bovet, S., Chandelier, L., Ilves, R., Klonus, S., Marshal, P., Schläpfer, D., Tabor, M., Thom, C., Veje, N., 2009. Digital airborne photogrammetry—a new tool for quantitative Remote Sensing?—A state-of-the-art review on radiometric aspects of digital photogrammetric images, Remote Sensing, vol. 1, pp. 577-605.
- Höhle, J., 2009a. DEM generation using a digital large-format frame camera, Photogrammetric Engineering & Remote Sensing (PE&RS), Vol. 75, no.1, pp. 87-93.
- Höhle, 2009b. Updating of the Danish elevation model by means of photogrammetric methods, National Survey and Cadastre-Denmark, technical report series, 03, ISBN87-92107-25-7, 64 p., [http://www.kms.dk/NR/rdonlyres/1C10C559-6CC9-4520-85C5DE8659CB38A9/0/kmsrep\\_3.pdf](http://www.kms.dk/NR/rdonlyres/1C10C559-6CC9-4520-85C5DE8659CB38A9/0/kmsrep_3.pdf) (accessed 23.4.2011).
- Minten, H., 2011. News from IGI, in: Fritsch, D. (Ed.), Photogrammetric Week '11, Wichmann Verlag, ISBN 978-3-87907-507-2, pp. 27-32.
- Neumann, K., 2011 The Z/I DMC II – “Imaging Revolution”, in: Fritsch, D. (Ed.), Photogrammetric Week '11, Wichmann Verlag, ISBN 978-3-87907-507-2, pp. 97-101.
- Sandau, R. (editor), 2005. Digitale Luftbildkamera, Einführung und Grundlagen, Wichmann Verlag, ISBN 3-87907-391-0, 342 p.
- Spreckels, V. Syrek, L., Schlienkamp, A., 2010. DGPF Project: Evaluation of Digital Photogrammetric Camera Systems – Stereoplotting, PFG 02/2010, pp.117-130.
- Trimble/Inpho, 2011. Reference manual of the software package Match-T DSM 5.4., <http://www.inpho.de/> (accessed 27.11.2011).